Mechanical-Motion-Rectifier-based Energy Harvester Using a Ball-screw Mechanism

Dr. N. Senthilvelan [1], P. Sivakumar[2], G. Rajamahendran[3], B. Ashok[4]

[1]*Professor, Department of Mechanical Engineering, Sembodai Rukmani Varatharajan Engineering College, Vedaranyam, Tamil Nadu, India*

[2,3,4]*Assistant professor, Department of Mechanical Engineering, Sembodai Rukmani Varatharajan Engineering College, Vedaranyam, Tamil Nadu, India*

Abstract—In this paper, a new-type of mechanical-motion- rectifier-based energy harvesting shock absorber using a ball-screw mechanism and two one-way clutches is proposed to replace conventional oil dampers in vehicle suspensions. The proposed energy-harvesting shock absorber can work as a controllable shock absorber as well as an energy harvester. The challenge to harvest energy from reciprocating suspension vibration is solved by integrating a mechanical motion rectifier (MMR) in the proposed design, which can convert reciprocating vibration into unidirectional rotation of a generator. As a result, the proposed shock absorber achieves high energy-harvesting efficiency by enabling the generator to rotate at a relatively steady speed during irregular vibrations and improves system reliability by reducing impact forces in transmission gears. In addition, the backlash of the proposed shock absorber is significantly reduced due to the use of the ball-screw mechanism, which further increases transmission durability and efficiency. Lab and field tests are carried out to experimentally characterize the proposed energy-harvesting shock absorber. The field testing results show that, when the modified vehicle is driven on a paved road at 40mph, the proposed energy-harvesting shock absorber is able to reduce the root-mean-square value of chassis acceleration by 11.12% over the oil shock absorber and simultaneously harvest an average power of 13.3W for a representative period of 8 seconds.

Keywords — Energy harvester, Semi-active shock absorber, Regenerative shock absorber, Inerter, Mechanical motion rectifier (MMR), ball-screw mechanism, One-way clutch

I. INTRODUCTION

vibration has been a serious concern in many large-scale vibration systems, such as vehicle suspensions, tall buildings, long-span bridges, etc. For instance, the vibration induced by road roughness in vehicle suspensions can cause discomfort to vehicle occupants and deteriorate vehicles' road handling. On the other hand, the associated vibration energy in these systems can be very large, which is worth being harvested to provide sustainable energy for many applications. In recent years, various energy harvesters have been developed to harvest energy from large-scale vibration sources, which can be generally classified into three main categories: linear energy harvesters [1-7], bidirectional rotary energy harvesters [8-12], and motion-rectifier-based energy harvesters [13-16]. Linear energy harvesters have a set of voice coils moving in an array of magnetic fields, which can produce electricity and a back electromotive force (EMF). Their energy-harvesting efficiency is generally high, but damping is too small. For instance, the linear energy-harvesting shock absorber proposed in [7] can achieve 70% - 78% mechanical efficiency, but it can only provide a damping of 940 Ns/m under a short circuitcondition, even not sufficient for a compact-sized passenger car. To overcome low-damping drawbacks, bidirectional rotary energy harvesters have been proposed, which utilize some mechanisms, such as ball screws [8-10], rack and pinions [11] or other motion conversion mechanisms [12], to transfer reciprocating linear vibration into bidirectional rotation of rotary generators to produce electricity. By converting low-speed linear motion into high-speed rotation, the damping of bidirectional rotary energy harvesters is significantly increased. However, the irregular oscillation of the motion transmission mechanism in bidirectional rotary energy harvesters causes numerous problems such as low efficiency and bad vibration performance. For example, the bidirectional rotary energy-harvesting shock absorber investigated in [11] has a suitable damping range of 1800Ns/m – 8000Ns/m, but it also has large backlash which leads to a relatively low mechanical efficiency of 33% - 56%.

Motion-rectifier-based energy harvesters [13-16] have been newly developed to convert reciprocating linear vibration into unidirectional rotation of generators and produce stable voltage with small ripples. Compared to bidirectional rotary energy harvesters, motion-rectifier-based design increases energy harvesting efficiency by enabling the generator to rotate at a relatively steady speed during irregular vibrations and improves system reliability by reducing impact forces in transmission gears. Li *et al* [13] developed a mechanical-motion-rectifier(MMR)-based energy-harvesting shock absorber using a rack-pinion mechanism with a mechanical efficiency of around 60%. However, backlash was still present in the rack-pinion mechanism located before the MMR. This backlash decreases energy-harvesting efficiency when it is subjected to small high-frequency vibration, commonly encountered in vehicle suspensions. In addition, racks and pinions are difficult to lubricate, which resulted in an exposed gear transmission system, significantly reducing the transmission durability and efficiency. Nagode *et al* [14] proposed a ball-screw-based MMR energy harvester to harvest the vibration from train suspensions. However, design in [14] adopted a planetary gear system and four one-way clutches to realize the motion rectification, which largely complicates the transmission system and causes additional friction easily

amplified by the ball screw mechanism. In addition, the damping and energy harvesting efficiency were not presented in [14]. The damping and mechanical efficiency of various types of energy harvesters are summarized in Table 1.

Table 1. Damping and mechanical efficiency of various types of energy harvesters

Types	Damping density	Mechanical efficiency
Linear[7]	Low	70%-78%
Bidirectional rotary[11]	High	33% - 56%
Rack-pinion MMR[13]	High	around 60%

In this paper, a new-type of mechanical-motion- rectifier-based energy harvesting shock absorber using a ball-screw mechanism and two one-way clutches is proposed to replace conventional oil dampers in vehicle suspensions. The proposed energy-harvesting shock absorber can work as a controllable shock absorber as well as an energy harvester. As a result, it has the potential to improve fuel efficiency [17] through harvesting the kinetic energy and achieve increased ride performance through self-powered suspension control [18-22]. Further design details are given in Section 2. It should be noted that the proposed MMR transmission system with the ball-screw mechanism can also be applied to efficiently harvest energy from a broad range of vibration sources, such as railcar and track vibration [23], wind-induced vibration in civil structures [24-25], etc.

In this paper, we also analyze the non-linear dynamics of the proposed energy-harvesting shock absorber induced by the engagement and disengagement of one-way clutches, which allow us to predict the rotational speed of the generator and the corresponding generated power. In addition to theoretical analysis, lab and field tests are also conducted to experimentally characterize the proposed energy-harvesting shock absorber.

This paper is organized as follows: Section II introduces the design and working principle. The dynamic modeling and theoretical analyses are presented in Section III. Lab and field tests are presented in Section IV and Section V, respectively. Finally, the paper is concluded in Section VI.

II. DESIGN AND WORKING PRINCIPLE

As shown in Figure 1, the proposed shock absorber consists of three modules: the ball screw, the enclosed MMR gearbox and the generator. The ball screw and nut are employed in back-driven mode, that is, low-speed reciprocating motion of the nut induced by irregular suspension vibrations drives the screw to bi-directionally rotate at high speed. The nut can move along the linear guide in the ball-screw case. Two eyelet connectors of the proposed shock absorber connect to the vehicle body and the wheel axle, respectively. To protect the proposed shock absorber from shock induced by road obstacles, the eyelet connectors are filled with rubber buffers which act as additional springs and dampers.

Compared to the rack-pinion mechanism [13], the ball-screw mechanism can significantly reduce backlash before the MMR, resulting in higher energy-harvesting efficiency. Also by using the ball-screw mechanism, an enclosed lubricated MMR gear transmission system can be designed, which increases the transmission durability and efficiency. In addition, sprag clutches adopted in the proposed design have much smaller backlash than that of the roller clutches used in the previous rack- pinion design [13]. However, the contact of the ball nut and screw causes additional friction. To reduce this friction, a highly lubricated large-lead screw is used in the proposed shock absorber.

The enclosed Mechanical Motion Rectifier (MMR) gearbox consists of one screw shaft, two one-way sprag clutches, two large and one small spiral bevel gears, bearings and lubricant sealing rings. The two one-way clutches are installed between

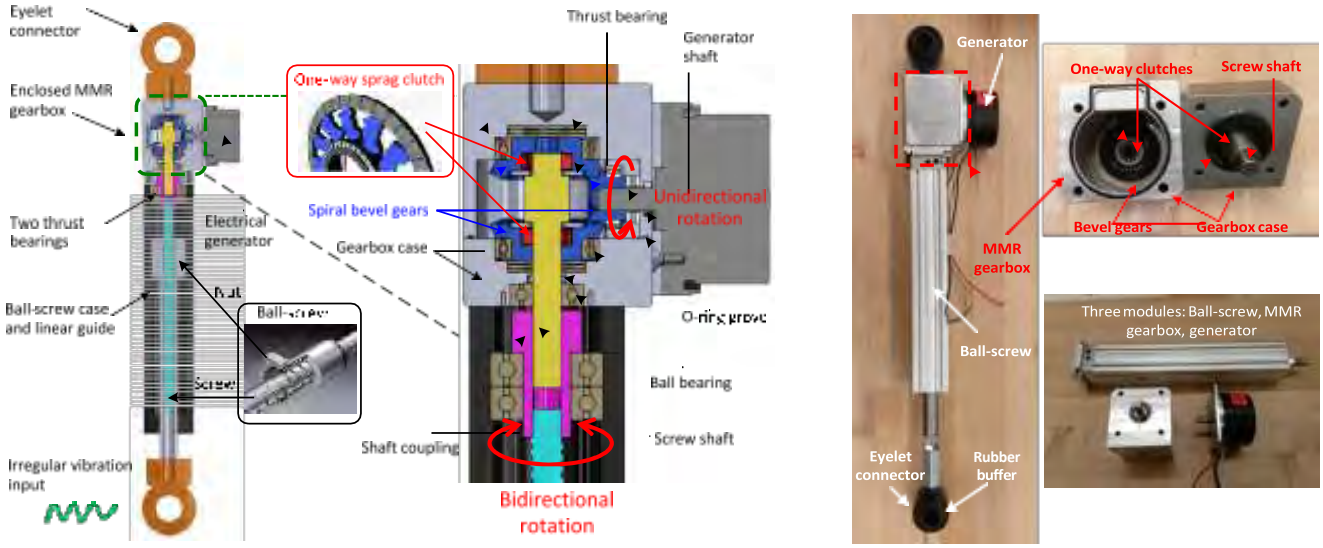

(a) (b)

Figure 1. The design of an MMR-based energy-harvesting shock absorber using a ball-screw mechanism (a) Design drawing (b) Built prototype

(a) (b)

Figure 2. The reciprocating suspension vibration will drive the electrical generator to rotate in one direction using the proposed ball-screw-based mechanical motion rectifier (MMR).

the screw shaft and the large gears, which can only transmit torque in one direction and idly rotate in the other direction, in a similar function as those used in bicycle gears. Due to these one-way clutches, at any instant in time only one large bevel gear is engaged to the screw shaft, becoming the driving gear. For instance, in Figure 2(a), if the screw shaft rotates counter-clockwise (as viewed from top to bottom), the lower clutch engages on the screw shaft and the lower gear becomes the driving gear to drive the generator to rotate clockwise (as viewed from left to right). During this period, the upper clutch is disengaged from the screw shaft and the upper gear idly rotates. Similarly, in Figure 2(b), clockwise rotation of the screw shaft also drives the generator to rotate clockwise, as the upper gear is now the driving gear and the lower gear is the idle gear. In this way, the generator always rotates in one direction no matter whether the proposed shock absorber extends or compresses.

Due to the conversion of reciprocating vibration into unidirectional rotation of the generator, the proposed transmission system is named a Mechanical Motion Rectifier (MMR) which is similar in a sense to electric voltage rectifiers used to regulate AC voltage into DC voltage. However, MMR's advantages go well beyond electric voltage rectifiers. The unidirectional rotation enables the generator to rotate steadily in its high-efficiency working condition from the oscillatory vibration of suspensions. Such a feature increases the energy conversion efficiency and reduces the impact force commonly caused by oscillatory motion.

The parameters of the prototype are listed in Table 2. The parameters selection is briefly summarized as follows. First, in order to maintain a high electrical efficiency, a nominal external resistance is chosen to be approximately 9 times larger than the internal resistance of the generator. With this total resistance, the gear transmission ratios (r_b, r_g), the screw lead and diameter (l and d_N) can be determined so that the nominal equivalent damping of the proposed shock absorber is suitable to the vehicles targeted. In this paper, we are targeting heavy-duty trucks or buses whose typical damping is around 8 - 10 kNs/m. The relation between the equivalent damping and the corresponding design parameters are derived in Equation (10) in Section III. In order to reduce friction and thus increase mechanical efficiency, the lead angle of ball screw $\lambda = \arctan(\frac{s}{nd_N})$ should be chosen as large as possible. Then the gear transmission ratio can be determined accordingly.

Table 2. The parameters of the prototype

Parameters	Value	description
d_N	8[mm]	Screw diameter
l	6[mm]	Ball-screw lead
f	0.15	Ball-screw friction factor
J_N	1.21 [kgcm^2]	Generator inertia
J_{Sg}	0.1[kgcm^2]	Large gear inertia
J_{cg}	0.0065[kgcm^2]	Small gear inertia
J_{bc}	0.02[kgcm^2]	Screw inertia
r_b	2	Bevel gear transmission ratio
r_g	1	Generator gearhead ratio
k_e	0.114 [V/rads]	Generator voltage constant
k_t	0.114 [Nm/A]	Generator torque constant
R_i	1.1 [ohm]	Internal resistance per phase
L	0.864[mH]	Internal inductance per phase
Length	600 [mm]	Shock absorber length
Strokes	150 [mm]	Shock absorber stroke
Weight	3.25 [Kg]	Shock absorber weight

III. MODELLING AND DYNAMICS

A. The dynamics of the generator

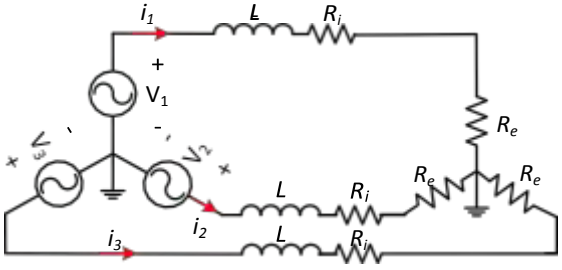

Figure 3. The dynamic model of a three-phase generator

A three-phase generator has been used in the proposed energy-harvesting shock absorber. In this paper, the energy-harvesting circuit is modeled as tunable external resistances, which can be lower than 1Ω [26]. Therefore, the dynamic model of the generator with the energy-harvesting circuit is modeled as shown in Figure 3, where V_1, V_2 and V_3

are the induced electromagnetic forces (EMF) generated by the respective phase of the generator. i_1 , i_2 and i_3 are the corresponding phase currents of the generator. L and R_i are the inductance and resistance of the voice coil per phase. R_e is the external resistive electrical load per phase.

The dynamics of the generator and its electrical damping have been analyzed in [11-12]. Neglecting the influence of the inductors, the resistive torque caused by electrical damping of the three-phase generator is [12]

$$v_{ENF} = \frac{3k_t k_e}{2R}\frac{d\theta}{dt} \quad (1)$$

where $R = R_i + R_e$, k_e and k_t are the voltage constant and torque constant of the generator, and θ is the angular displacement of the generator. To make the model more accurate, the friction of the generator including both Coulomb friction and viscous damping is also taken into account, which can be written as

$$v_{fric} = c_v\frac{d\theta}{dt} + v_0 sgn\left(\frac{d\theta}{dt}\right) \quad (2)$$

where v_{fric} is the friction torque of the generator, c_v is the viscous damping coefficient, and $v_0 sgn\left(\frac{d\theta}{dt}\right)$ is the Coulomb friction torque indicating that the friction torque opposes the direction of motion (sgn($\frac{d\theta}{dt}$) just returns the sign of $\frac{d\theta}{dt}$). According to Newton's law, the rotor's acceleration, $\frac{d^2\theta}{dt^2}$, is proportional to the total torque applied on the rotor of the generator

$$v_N - v_{ENF} - v_{fric} = J_N\frac{d^2\theta}{dt^2} \quad (3)$$

where v_N is input mechanical torque, J_N is rotor's rotational inertia. Substituting Equations (1) and (2) into Equation (3), the torque of the generator can be expressed as

$$v_N = J_N\frac{d^2\theta}{dt^2} + c_N\frac{d\theta}{dt} + v_0 sgn\left(\frac{d\theta}{dt}\right) \quad (4)$$

where c_N is the equivalent torsional damping of the generator contributed by both electrical and viscous damping

$$c_N = \frac{3k_t k_e}{2R} + c_v \quad (5)$$

The Coulomb friction torque v_0 is usually very small and negligible in most of generators. Therefore, the torque of the generator can be simplified as a torsional inertance J_N in parallel with a torsional damping $c_N = \frac{3k_t k_e}{2R} + c_v$.

B. The dynamics of the proposed shock absorber

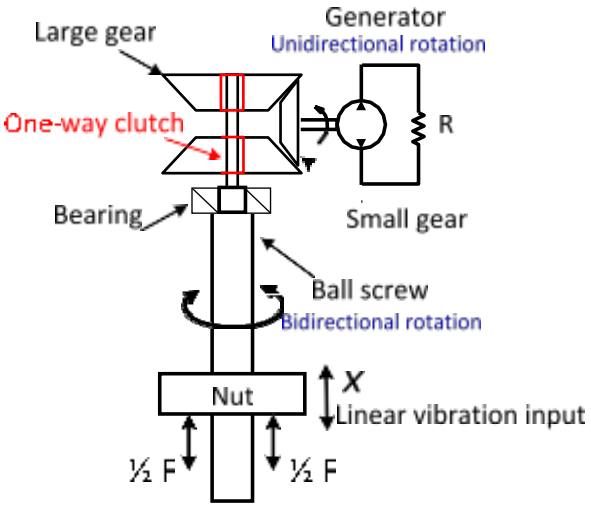

Figure 4. The dynamic model of the proposed energy-harvesting shock absorber

Figure 4 shows the dynamic model of the proposed shock absorber. Unlike linear and bidirectional rotary energy harvesters [1-12], the MMR-based energy-harvesting shock absorber has non-linear behaviors induced by the one-way clutches. When the rotational speed of the screw shaft is smaller than that of the large bevel gears, the one-way clutches inside the large gears disengage from the screw shaft, resulting zero torque transmission. On the other side, when the system is engaged, the screw shaft v_{bc} drives the system including the MMR gear transmission system and the generator. Therefore, during the engaged period,

$$\frac{d\theta}{dt} = \frac{d\theta_{in}}{dt} \quad (6)$$

where $\frac{d\theta_{in}}{dt} = \frac{r_b r_g}{s}\left|\frac{ds}{dt}\right|$ is defined as input rotational speed. x is the linear relative displacement of the shock absorber and l is the screw lead. r_b and r_g are the transmission ratios of the bevel gears and planetary gears. The thrust force F_e applied on the ball nut is proportional to the torque v_{bc} of the screw shaft [27]

$$F_e = \frac{2c_{bc}}{d_N}\left(\frac{nd_N + fs}{s - nfd_N}\right) \quad (7)$$

where d_N is the pitch diameter of the screw and f is the friction coefficient. Considering gear transmissions, the thrust force of the engaged shock absorber can be expressed as

$$F_e = \left[\left(\frac{nd_N + fs}{s - nfd_N}\right)\frac{2(r_b^2 r_g^2 J_N + r_b^2 J_{cg} + 2J_{lg} + J_{bc})}{s}\right]\frac{d^2s}{dt^2} + \left[\left(\frac{nd_N + fs}{s - nfd_N}\right)\frac{2r_b^2 r_g^2}{d_N s}\left(\frac{3k_t k_e}{2R} + c_v\right)\right]\frac{ds}{dt} \quad (8)$$

where J_{cg}, J_{sg} and J_{bc} are the rotational inertias of the small gear, large gear and screw shaft, respectively. Equivalently, the engaged shock absorber acts as a linear fixed inerter in parallel with a linear variable damper whose damping is tuned by the

electrical load of the generator. The equivalent inertance and damping are

$$N_e = \left(\frac{nd_N + fS}{S - nfd_N}\right)\frac{2(r_b^2 r_g^2 J_N + r_b^2 J_{cg} + 2J_{lg} + J_{bc})}{d_N S} \approx \left(\frac{nd_N + fS}{S - nfd_N}\right)\frac{2r_b^2 r_g^2 J_N}{d_N S} \quad (9)$$

$$c_e = \left(\frac{nd_N + fS}{S - nfd_N}\right)\frac{2r_b^2 r_g^2 3k_t k_e}{d_N S}\left(\frac{}{2R}\right) + c_v \quad (10)$$

In Equation (9), the contribution of the rotational inertias of the gears and screw, $r_b^2 J_{cg} + 2J_{Sg} + J_{bc}$, is much smaller than that of the generator $r_b^2 r_g^2 J_N$, which is especially true when the transmission ratios r_b and r_g are large. For instance, in the proposed design, $r_b^2 r_g^2 J_N = 4.82 kgcm^2$ is approximately 20 times larger than $r_b^2 J_{cg} + 2J_{Sg} + J_{bc} = 0.246 kgcm^2$. Therefore, the equivalent inertance N_e of the shock absorber is mainly dominated by the rotational inertia of the generator and $r_b^2 J_{cg} + 2J_{Sg} + J_{bc}$ is negligible.

When the input rotational speed is smaller than the rotational speed of the generator, disengagement of the MMR occurs.

$$\frac{d\theta_{in}}{dt} < \frac{d\theta}{dt} \quad (11)$$

During the disengaged period, the generator drives the gear transmission system at a higher speed than that of the screw shaft due to the kinetic energy stored in the inertia of the mechanical elements, such as gears or the rotor of the generator. While this occurs, the screw shaft does not transmit any torque to the generator and thus the force of the shock absorber is just zero

$$F_d = 0 \quad (12)$$

However, this rotational speed will gradually decrease due to the electrical load of the generator, which converts kinetic energy into electricity. When the input rotational speed θ_{in} is equal to the rotational speed of the generator $\dot{\theta}$ again, the one-way clutches get re-engaged and start transmitting torque to the generator.

To sum up, the force of the proposed MMR-based shock absorber is given by

$$\begin{cases} F_e = N_e \frac{d^2 s}{dt^2} + c_e \frac{ds}{dt} & \dot{\theta} = \dot{\theta}_{in}, \text{ engaged period} \\ F_d = 0 & \dot{\theta} > \dot{\theta}_{in}, \text{ disengaged period} \end{cases} \quad (13)$$

where N_e and c_e can be solved from Equation (9) and (10). It is worth noting that all the mechanical energy in the primary suspension system will be kept conservatively during the disengaged period since the primary system becomes an undamped system. Ideally, the proposed design won't cause additional mechanical energy loss during disengaged period.

C. The rotational speed of the generator and the generated power

Since any arbitrary vibration inputs can be decomposed into a series of sinusoidal vibration inputs, the proposed shock absorber is analysed when subjected to sinusoidal vibration inputs.

$$x = A\sin(mt) \quad (14)$$

where A is the amplitude and m is the angular frequency of the sinusoidal vibration input.

As explained above, when the MMR is disengaged, the torque of the screw shaft v_{bc} is zero. Neglecting the rotational inertia of the gears, the governing equation of the generator during the disengaged period can be obtained as

$$J_N \frac{d^2\theta}{dt^2} + c_N \frac{d\theta}{dt} = 0 \quad (15)$$

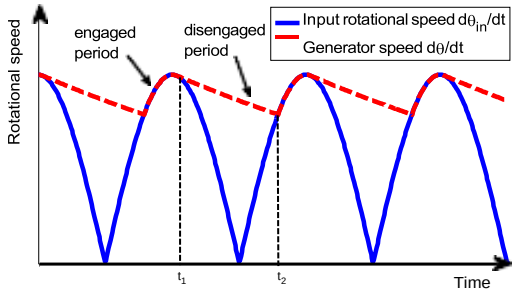

Figure 5. The switching of engagement and disengagement inside the mechanical motion rectifier. $\theta_{in} = \frac{r_b r_g}{S}|x|$ and θ is the angular displacement of the generator.

Figure 5 shows the switching dynamics of the engagement and disengagement of the MMR. At t_1,

$$\frac{d\theta}{dt} = \frac{d\theta_{in}}{dt} \quad (16)$$

and the one-way clutch starts disengaging from the screw shaft. At this time, the input angular acceleration can be obtained from Equation (14)

$$\frac{d^2\theta_{in}}{dt^2} = \frac{r_b r_g}{S}\frac{d^2 s}{dt^2} = -\frac{r_b r_g}{S} Am^2 \sin(mt_1) \quad (17)$$

and the angular acceleration of the generator is

$$\frac{d^2\theta}{dt^2} = -\frac{c_N}{J_N}\frac{d\theta}{dt} = -\frac{c_N}{J_N}\frac{d\theta_{in}}{dt} = -\frac{c_N}{J_N}\frac{r_b r_g}{S} Am\cos(mt_1) \quad (18)$$

When disengagement occurs at t_1,

$$\frac{d^2\theta_{in}}{dt^2} \le \frac{d^2\theta}{dt^2} \quad (19)$$

Substituting Equations (17) and (18) into Equation (19), t_1 can be calculated as

$$t_1 = \frac{1}{m}\arctan\left(\frac{c_N}{mJ_N}\right) + \frac{Kn}{m}, \qquad K = 0,1,2,3\cdots \qquad (20)$$

where K is a series of different integers standing for the disengaged instant in every half time period. During the disengaged period, the rotation of the generator is governed by Equation (15). Therefore the rotational speed of the generator during the disengaged period can be obtained as

$$\frac{d\theta}{dt} = \frac{d\theta}{dt}(t_1) * e^{\frac{-c_N}{J_N}(t-t_1)}, \quad t_1 \le t \le t_2 \qquad (21)$$

where $\frac{d\theta}{dt}(t_1) = \frac{r_b r_g}{S} Am|\cos(mt_1)|$. When the system becomes re-engaged at t_2, the rotational speed of the generator is equal to $\frac{d\theta_{in}}{dt}$. Therefore, at t_2,

$$\cos(mt_1)\, e^{\frac{c_N}{J_N}t_1} + \cos(mt_2)\, e^{\frac{c_N}{J_N}t_2} = 0, \; t_1 \le t_2 \le t_1 + \frac{n}{m} \qquad (22)$$

Then, the corresponding t_2 can be solved from Equation (22) for every t_1 with a different K. To sum up, the rotational speed of the generator is governed by the following equations

$$\begin{cases} J_N \frac{d^2\theta}{dt^2} + c_N \frac{d\theta}{dt} = \frac{d\theta_{in}}{dt} & t_2 \le t \le t_1 \\ \frac{d\theta}{dt} = 0 & t_1 < t < t_2 \end{cases} \quad K = 0,1,2,3\cdots \qquad (23)$$

where t_1 and t_2 with different K are solved from Equations (20) and (22).

Once the rotational speed of the generator is obtained, the generated phase voltage is $k_e \frac{d\theta}{dt}$ and the electrical power envelop per phase can be solved by

$$P_e = \frac{k_e^2}{R}\left(\frac{d\theta}{dt}\right)^2 \qquad (24)$$

IV. LAB TESTS AND ANALYSIS

A. Experimental setup

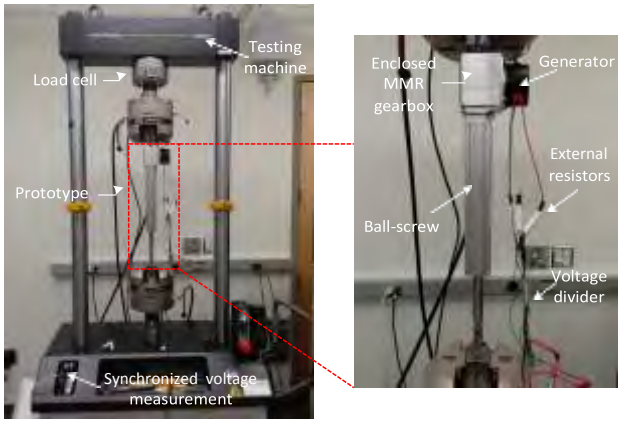

Figure 6. Experimental setup

As shown in Figure 6, the shock absorber prototype was tested on an Instron testing machine which has a built-in load cell and a displacement sensor to record the force and displacement data. A series of sinusoidal inputs, with frequencies ranging from 1Hz to 10 Hz and amplitudes ranging from ±0.5mm to ±5mm, were used to excite the shock absorber prototype during the tests. The external electrical loads were connected to the three-phase generator in a "Y" configuration [28], as shown in Figure 3. A 1-to-41 voltage divider was used to measure the voltage across the external resistors. The damping and energy-harvesting characteristics of the shock absorber prototype are presented in the following subsections.

B. Force-displacement loops and damping characteristics

Since suspensions experience vibration over a broadband spectrum, mainly 1-10Hz [29], the performance of the proposed shock absorber was investigated for various excitation frequencies ranging from 1Hz to 10Hz.

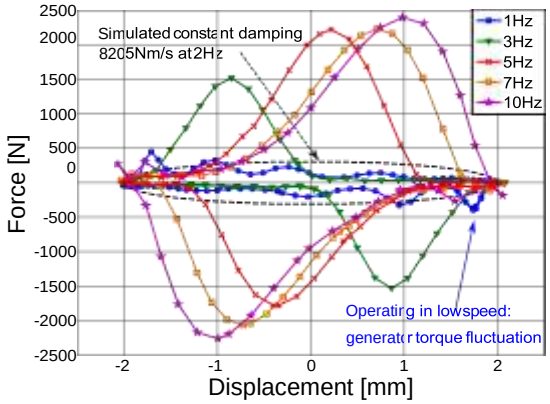

(a)

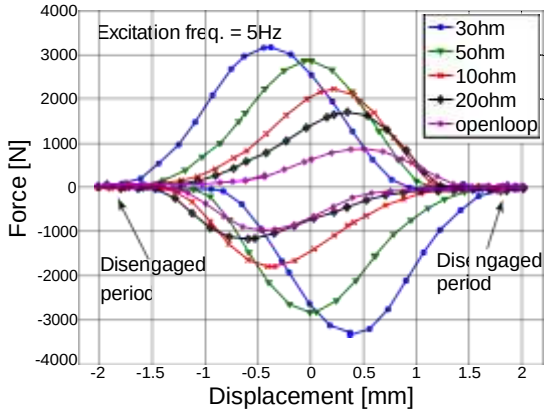

(b)

Figure 7. Force-displacement loops under harmonic vibration inputs of $A = \pm 2mm$. (a) for different excitation frequencies with external electrical load $R_e = 10\Omega$. (b) for different external electrical loads with frequency 5Hz.

Figure 7 shows the force-displacement loops of the proposed shock absorber for different excitation frequencies and external electrical loads. Figure 7(a) shows the force-displacement loops under harmonic vibration inputs of 2mm amplitude with 10Ω

electrical loads. The results indicate that the shock absorber starts engaging earlier as the excitation frequency decreases, which corresponds to a shorter disengaged period $t_2 - t_1$. This also explains why the peak force is shifted from the left to the right as the excitation frequency increases. In Figure 7(a), the fluctuation of the damping force is observed at 1Hz excitation frequency. This is because the generator rotates at low speed when the vibration input is slow, which causes torque fluctuation due to an uneven distribution of the magnets inside the generator. In order to reduce this fluctuation, the gear transmission ratio can be increased so that the generator also rotates at relatively high speed even under low-frequency excitations. It should be noted that the damping characteristics of MMR-based shock absorbers are different from those of conventional dampers. The disengagement of the one-way clutches and the additional inertia force can possibly improve suspension performance in terms of ride comfort, road handling, suspension stroke, etc., as reported in [30].

Figure 7(b) shows force-displacement loops under harmonic vibration inputs of 5Hz frequency and $\pm$2mm amplitude. The results show that the forces reduce to zero before the displacements reach their maximum or minimum. This is because the kinetic energy stored in the generator inertia is returned to the system and the one-way clutch disengages during disengaged periods, agreeing with the analysis in Section III. Moreover, the results indicate that the smaller the electrical load, the shorter the disengaged period. This is because the equivalent damping of the shock absorber grows as the electrical load decreases. The larger damping causes the generator to slow down faster during the disengaged periods and thus the generator will be reengaged to the system in a shorter time period.

In Figure 7, the area of the force-displacement loop represents the mechanical work input of the shock absorber ΔW during one work cycle. Therefore, the mechanical power input can be obtained by [11]

$$P_N = f * \Delta W \tag{25}$$

where f is the frequency of the vibration input. Moreover, the equivalent damping coefficient can be calculated as [11]

$$c_{eq} = \frac{\Delta M}{2\pi f X} \tag{26}$$

where X is the amplitude of the harmonic vibration input. Based on Equation (26), the equivalent damping of the shock absorber prototype is calculated for different electrical loads under vibration inputs of 2Hz frequency close to the first resonance of vehicle suspensions, as shown in Figure 8.

The results show that the smaller the electrical load, the larger the damping force and damping coefficient. Figure 8 also shows that a minimum damping of 4425 Ns/m is achieved when the shock absorber is in open-loop status. This means the damping of the shock absorber contributed by the viscous damping of the generator $c_v \left(\frac{n d_N + f S}{S - n f d_N}\right)^2 \frac{r^2 r^2}{b g} = 4425$ Ns/m. Then the damping of the shock absorber can be properly predicted, as is also plotted in Figure 8. The results also show that the damping of the shock absorber with a 10Ω electrical load is 8205Ns/m, a damping value typically suitable to trucks or buses. In addition, Figure 8 shows the damping range of the proposed shock absorber is 4.43kNs/m – 15.42kNs/m, which can be changed by adjusting the electrical loads, or adjusting the duty-cycle of DC/DC energy converter in the energy harvesting circuit [31]. As a comparison, a typical suspension damping for passenger cars is 1.5kNs/m [20], and for heavy-duty trucks or buses is 8-10kNs/m [32-33].

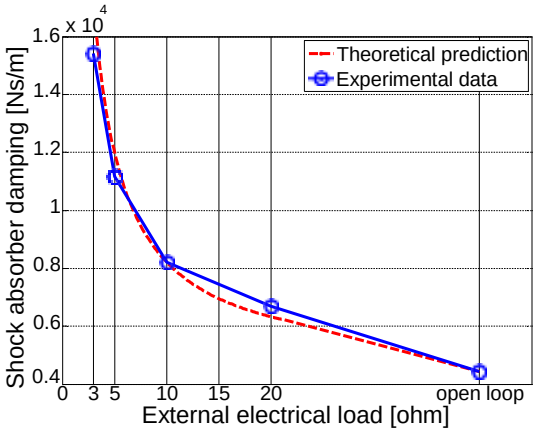

Figure 8. Equivalent damping for different electrical loads under vibration inputs of 2Hz frequency.

C. Energy harvesting and efficiency

The generated voltage V per phase was recorded during the tests and the instantaneous electrical power per phase can be calculated as

$$P_c = \frac{V^2}{R} \tag{27}$$

where V is the instant phase voltage. The average of total power generated by the three-phase generator over a time period T can be obtained as

$$P_{ave} = 3 \times \frac{\int_0^T P_c dt}{T} \tag{28}$$

Figure 9 show the simulated and measured electrical power per phase together with the shock absorber force under harmonic excitations with 4Hz frequency, 10+1.1=11.1 Ω total electrical load and $\pm$2mm amplitude. Under such a condition, the maximum phase power is around 11.52 watts and the average phase power is 2.25 watts. Figure 9(b) also shows that the proposed shock absorber can stabilize the rotational speed of the generator to never fall to zero as occurs in linear and bidirectional rotary energy harvesters [1-12]. The asymmetric shape of the generated power is also observed, as the slope of the generated power is larger when increasing than when decreasing.

Note that the power increases as the amplitude and the frequency of vibration inputs increase.

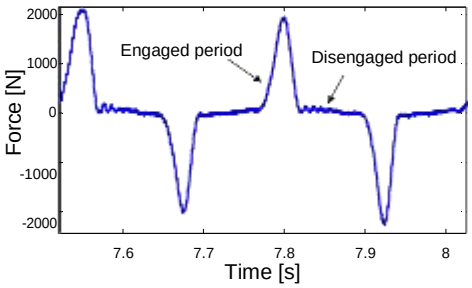

(a)

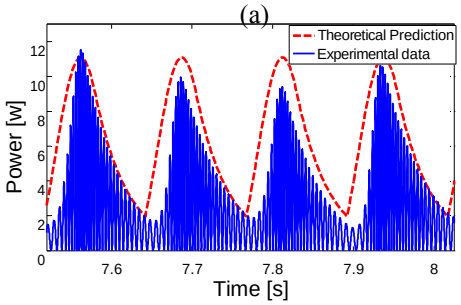

(b)

Figure 9. (a) Measured force (b) Measured and Simulated phase power under harmonic excitations with 4Hz frequency, $R_i + R_e$ =11.1 Ω total electrical load and ±2mm amplitude. (Max. power = 11.52 W, Ave. power = 2.25W)

The total energy-harvesting efficiency can be decomposed into the electrical efficiency 5_e and the mechanical efficiency 5_N. The electrical efficiency is the ratio of power on the external electrical load to the total electrical power, which is R_e divided by total resistance $R_e + R_i$. The mechanical efficiency is defined as the ratio of total electrical power to mechanical input power. The mechanical and electrical efficiency of the proposed shock absorber under different working conditions are shown in Figure 10. Figure 10 (a) shows the mechanical and electrical efficiency for different external electrical loads R_e = 3~20Ω and different amplitudes A = ±1~ ± 5NN of 2Hz harmonic excitations. The internal resistance of the generator R_i = 1.1Ω and the electrical efficiency 5_e is 73.2% ~ 94.7% for R_e = 3~20Ω. The mechanical efficiency 5_N increases as the electrical load decreases or the excitation amplitude increases. For A = ±2NN, the mechanical efficiency increases from 27% to 57.9% as R_e decreases from 20Ω to 3Ω. The corresponding total energy harvesting efficiency ranges from 25.6% to 42.4%.

Figure 10(b) shows the mechanical efficiency for different excitation frequencies 1-5Hz with different external electrical loads R_e = 3~10Ω . The results show that the mechanical efficiency increases as the excitation frequency increases. For R_e = 3Ω, the total energy harvesting efficiency ranges from 35.9% to 51.9%. The highest mechanical efficiency 70.1% is achieved at 4Hz frequency and R_e = 3Ω. It should be noted that there are trade-offs between damping performance and energy-harvesting performance. The maximum damping of the shock absorber is achieved when the generator is short-circuited, but in this case, the harvested energy would be zero. However, the maximum damping may not be the desired damping in vehicle suspension systems. The trade-offs between energy harvesting performance and suspension performance have to take into account the coupled dynamics of the vehicle suspension with the proposed shock absorber, as has been comprehensively studied in [30].

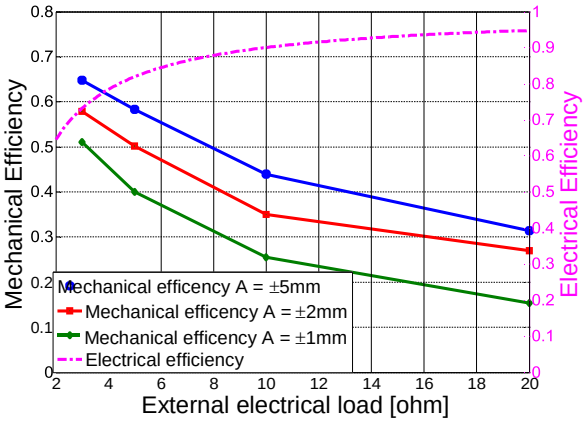

(a)

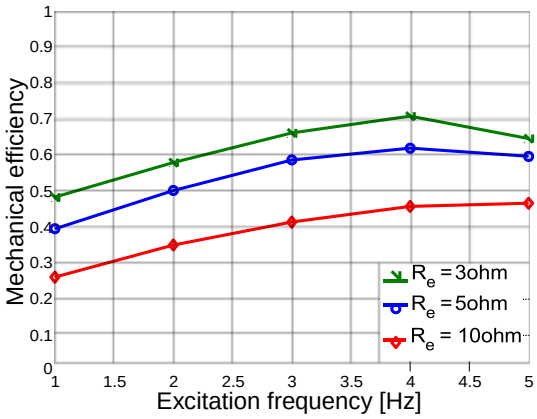

(b)

Figure 10. Mechanical efficiency (a) for different electrical loads and different amplitudes under vibration inputs of 2Hz frequency, (b) for different excitation frequencies and different electrical loads under vibration inputs of ±2mm amplitude.

D. Efficiency comparison of ball-screw-based MMR shock absorber and rack-pinion-based MMR shock absorber [13]

Figure 11 shows the comparison of the mechanical efficiency between the ball-screw-based MMR shock absorber and rack-pinion-based design [13] under harmonic vibrations with different amplitudes and electrical loads. To make a fair comparison, a test was done with both harvesters in which the electrical efficiency of these two types of MMR-based shock absorbers were kept the same. To do this, the external load of the rack-pinion MMR shock absorber was 6 times larger than that of the proposed ball-screw-based shock absorber. It is observed that the mechanical efficiency of the rack-pinion shock absorber dramatically decreases as the vibration amplitude decreases, and ceases to work in excitations below A = ±0.5mm due to the backlash between the rack teeth and

pinion teeth. However, the ball-screw shock absorber can still generate power under small excitation conditions. This low-backlash feature can increase the energy harvesting efficiency of the proposed shock absorber, especially when being used on smooth highways. The results in Figure 11 also show that the proposed ball-screw-based MMR shock absorber has higher efficiency when the electrical load is small, which is suitable to harvest energy from heavy-duty vehicles with large suspension damping.

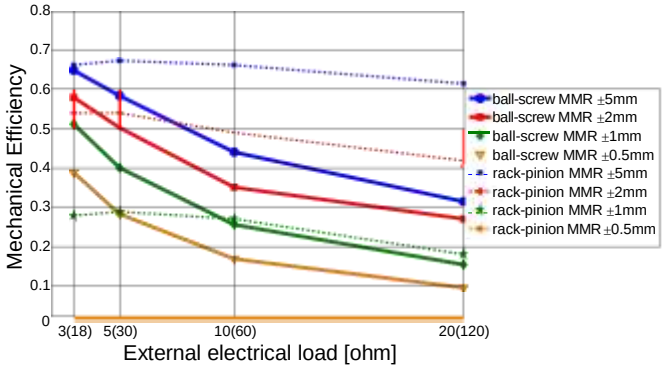

Figure 11. Mechanical efficiency of the ball-screw-based MMR energy harvester (solid line) and rack-pinion-based MMR energy harvester [13] (dotted line) under harmonic vibration inputs with ±0.5mm to ±5mm amplitude and 2Hz frequency.

However, the mechanical efficiency of the proposed design is lower than the rack-pinion design at higher electrical resistances. The reason is as follows. First, the total energy-dissipating force of the shock absorber is composed of electrical damping forces and mechanical friction forces. The work only done by the electrical damping force can be converted to the electrical energy. The mechanical friction force of the proposed design is larger than that of the rack-pinion design due to additional friction induced by the ball screw and the high-speed rotational MMR gearbox. Under high electrical resistances, the electrical damping force is small and the total energy-dissipating force is dominated by the mechanical friction force. As a result, for the proposed design, the ratio of power lost due to mechanical friction to the input power is larger than that of the rack-pinion design, resulting in a lower mechanical efficiency. However, as electrical resistance decreases, the electrical damping force increasingly contributes to the total energy-dissipating force, bringing the mechanical efficiency of both designs closer. In addition, the backlash of the proposed design is smaller than the rack-pinion design. Therefore, with small electrical resistances, the proposed ball-screw design can have higher mechanical efficiency than the rack-pinion one, especially when vibration inputs are small (≤1mm).

V. FIELD TESTS

Field tests were also carried out to further validate the feasibility of the proposed energy-harvesting shock absorber, as shown in Figure 12. Figure 12 (a) shows the test setup in which the proposed shock absorber prototype was installed on a Ford F250 pick-up truck to replace its original left-rear oil damper. A 300kg weight was also loaded in the truck bed to emulate an actual truck-loaded situation. A laser displacement sensor and an accelerometer were used to record suspension displacement and chassis acceleration. The tests were conducted by driving the modified vehicle at 40mph on a paved road near Virginia Tech campus. For comparison purpose, the chassis acceleration of the vehicle with its original shock absorber was also measured under the same testing condition.

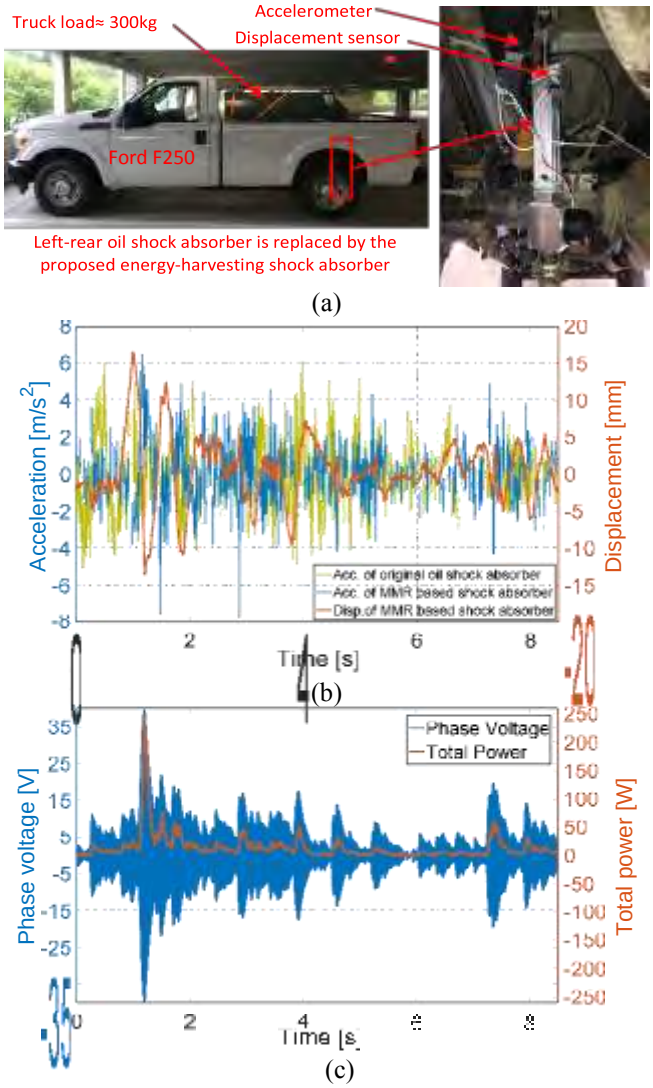

Figure 12. (a) Setup of field tests (b) Suspension displacement and chassis acceleration in comparison with chassis acceleration of the vehicle with its original oil shock absorber. (c) Phase voltage and corresponding total power of the generator. Testing condition: 40mph and 10Ω resistors.

Figure 12(b) shows the suspension displacement and chassis acceleration of the modified vehicle in comparison with the chassis acceleration of the vehicle with its original shock absorber for a representative period of 8 seconds. To maximize ride comfort instead of energy harvesting, 10Ω electrical loads were connected to the proposed shock absorber, of which the

mechanical efficiency is 35.1% under harmonic inputs with 2Hz frequency and 2mm amplitude. As a result, the RMS value of the chassis acceleration of the MMR-based vehicle is $1.45\mathrm{m/s^2}$, which is 11.12% smaller than that of the original vehicle. It should be mentioned that a low pass filter with a cut-off frequency 100Hz and stopband frequency 200Hz was used to filter out high-frequency measurement noises for both acceleration data.

The corresponding energy harvesting performance is plotted in Figure 12(c). The results show that the average total power generated per shock absorber is 13.3W for the 8-second period, which proves that the proposed shock absorber can continuously generate a usable amount of energy from suspension vibration of vehicles driven on paved roads. In addition, in order to increase energy harvesting performance, 3 Ω resistors were also connected to the proposed shock absorber during the tests, an average power of 24.7 W can be obtained under the same driving condition.

VI. Conclusion

In this paper, a new-type of MMR-based energy-harvesting shock absorber using a ball-screw mechanism and two one-way clutches is proposed. Due to the one-way clutches, the proposed shock absorber is able to convert reciprocating suspension vibration into the unidirectional rotation of a generator. This function not only achieves high energy-harvesting efficiency by enabling the generator to rotate at a relatively steady speed during irregular vibrations, but also improves the system reliability by reducing impact forces in transmission gears. The non-linear dynamics of the MMR mechanism induced by the one-way clutches is also analysed. It is shown that the engaged shock absorber acts as a fixed inerter in parallel with a variable damper tuned by the electrical loads of the generator.

In addition to theoretical analysis, lab tests are conducted to experimentally characterize the proposed shock absorber. It is found that the equivalent damping increases from 4,425Ns/m to 15,420 Ns/m as the electrical load changes from open loop to 3Ω under harmonic excitations. The energy-harvesting efficiency of the proposed shock absorbers is also studied for various working conditions. The highest mechanical efficiency of 70.1% and the corresponding 51.9% energy harvesting efficiency are achieved under 4Hz harmonic vibration input with 3Ω external electrical loads. Moreover, it is found that the backlash of the proposed shock absorber is much smaller than the existing rack-pinion design. Finally, field tests are carried out to further validate the feasibility of the proposed energy-harvesting shock absorber. The results show that, when the modified vehicle is driven on a paved road at 40mph, the proposed energy-harvesting shock absorber is able to reduce the root-mean-square value of chassis acceleration by 11.12% over the oil shock absorber and simultaneously harvest an average power of 13.3W for a representative period of 8 seconds.

References

[1] Karnopp, D., "Permanent magnet linear motors used as variable mechanical dampers for vehicle suspensions," Vehicle System Dynamics, vol. 18, no. 4, pp.187–200, 1989.

[2] Goldner, R.B., Zerigian, P. and Hull, J.R., "A preliminary study of energy recovery in vehicles by using regenerative magnetic shock absorbers," Paper SAE 2001-01-2071, SAE/DOE Government/Industry Meeting, Washington, DC, 2001

[3] Gupta, A., Jendrzejczyk, J.A., Mulcahy, T.M. and Hull, J.R., "Design of electromagnetic shock absorbers," International Journal of Mechanics and Materials in Design, vol 3, no 3, pp. 285–291, 2006.

[4] Martins, I., Esteves, J., Marques, G.D. and Silva, F.P.D., "Permanent-magnets linear actuators applicability in automobile active suspensions," IEEE Transaction on Vehicular Technology, vol. 55, no. 1, pp. 86–94, 2006.

[5] Zuo, L., Scully, B., Shestani, J. and Zhou, Y., "Design and characterization of an electromagnetic energy harvester for vehicle suspensions," Smart Material and Structures, vol. 19, no. 4, pp. 045003, 2010

[6] Chen, C. and Liao, W.H., "A self-sensing magnetorheological damper with power generation," Smart Material and Structures, vol. 21, no. 2, pp. 025014, 2012

[7] Tang, X., Lin, T. and Zuo, L., "Design and optimization of a tubular linear electromagnetic vibration energy harvester," IEEE/ASME Transactions on Mechatronics, vol. 19, no.2, pp.615-622, 2014.

[8] Zhang, Y., Huang, K., Yu, F., Gu, Y., and Li, D., "Experimental verification of energy-regenerative feasibility for an automotive electrical suspension system," Vehicular Electronics and Safety. ICVES. IEEE International Conference on, pp. 1-5, 2007

[9] Kawamoto, Y., Suda, Y., Inoue, H. and Kondo, T., "Electro-mechanical suspension system considering energy consumption and vehicle maneuver," Vehicle System Dynamics, vol. 46, no. S1, pp.1053-1063, 2008

[10] Cassidy, I.L., Scruggs, J.T., Behrens, S. and Gavin, H.P. "Design and experimental characterization of an electromagnetic transducer for large-scale vibratory energy harvesting applications," Journal of Intelligent Material Systems and Structures, vol. 22, no.17, pp.2009-2024, 2011.